Open File Envelope No. 9636

EL 2578

SANDILANDS

FIRST ANNUAL AND FINAL REPORT FOR THE PERIOD 27/1/99 TO 26/1/00

Submitted by

BHP Minerals Pty Ltd
2000

Enquiries: Customer Services
Ground Floor
101 Grenfell Street, Adelaide 5000

Telephone: (08) 8463 3000
Facsimile: (08) 8204 1880

PRIMARY INDUSTRIES AND RESOURCES SA

CR 9797

EL 2578
SANDILANDS
SOUTH AUSTRALIA

FIRST ANNUAL AND FINAL REPORT FOR THE PERIOD ENDED 26 JANUARY 2000

Spatial data included in this report
is based on the AGD66 Datum

Prepared by:
Matthew White
Consultant Geologist
White Geoservices Pty Ltd

Submitted by:

Jeremy Read
Team Leader

BRISBANE
APRIL 2000

BHP Minerals Pty. Ltd., A.C.N. 008 694 782

CR 9797

EL 2578
SANDILANDS
SOUTH AUSTRALIA

FIRST ANNUAL AND FINAL REPORT
FOR THE PERIOD ENDED
26 JANUARY 2000

M WHITE

APRIL 2000

DISTRIBUTION:

Department of Primary Industry and Resources SA	(2)
BHP Minerals Brisbane Library (PDF)	(1)
BHP Minerals Eastern Proterozoic Group	(1)

TABLE OF CONTENTS

LIST OF FIGURES

LIST OF TABLES

LIST OF APPENDIXES

SUMMARY

This report summarises the exploration work carried out by BHP Minerals Pty Ltd (BHPM) on EL 2578, during the annual period to 26 January 2000.

Exploration work carried during the period consisted of the following:

- a 25 Hz GEOTEM survey;
- an assessment of the GEOTEM results and other magnetic anomalies.

No field work was undertaken on EL 2578 during the period. No high priority targets were observed in the GEOTEM survey results or aeromagnetic anomalies. Consequently, EL 2578 was surrendered on 26 January 2000.

1. INTRODUCTION

This annual and final report summarises the exploration work carried out by BHP Minerals Pty Ltd (BHPM) on EL 2578 during the annual period to 26 January 2000. The tenement was granted on 27 January 1999 and only held for 12 months, due to a lack of encouraging results (see below).

EL 2578 is located on the eastern side of the Yorke Peninsula of South Australia. The tenement covers an area of 525 km^2 (**Figure 1**).

The principal targets for EL 2578 are:
1) iron oxide Cu-Au mineralisation (IOCG) similar to Olympic Dam; and
2) Broken Hill Type (BHT) stratiform Pb-Zn-Ag mineralisation.

Tenement expenditure for the period is detailed in **Appendix 1.**

2. EXPLORATION STRATEGY

EL 2578 was granted to BHPM on 27 January 1999, to cover a GEOTEM anomaly from BHPM's Moonta survey flown in 1988. The tenement also covers the Curramulka magnetic complex further south. Both these target areas were assessed during the period.

3. PREVIOUS WORK

Previous exploration in the area for base metals, uranium and coal in the 1980s was extensive, particularly by Esso and BHP (ELs 255, 499, 906, 1112 – Curramulka Project). Previous work includes seismic lines, gravity surveys, aeromagnetics, regional drilling traverses and diamond drilling.

One interesting aeromagnetic anomaly was tested by BHP on the eastern part of the licence area. This magnetic target lies along the major NNE striking structure along the east side of the Yorke Peninsula. The hole (PJ1A) intersected strongly albite – red rock – magnetite altered rock with strong brecciation, and carbonate and actinolite alteration, with minor pyrite and chalcopyrite.

An assessment of the Curramulka magnetic complex showed that previous drilling did not test one of the best magnetic anomalies within the complex. The nearest hole is CURD4 (collared by BHP some 600 m north of the northern tip of the magnetic anomaly). The hole intersected a red rock altered gneiss, with disseminated magnetite, plus some areas of pervasive ?amphibole/ chlorite, carbonate alteration with pyrite. The rock was not strongly brecciated. This potential target was considered for further follow up work.

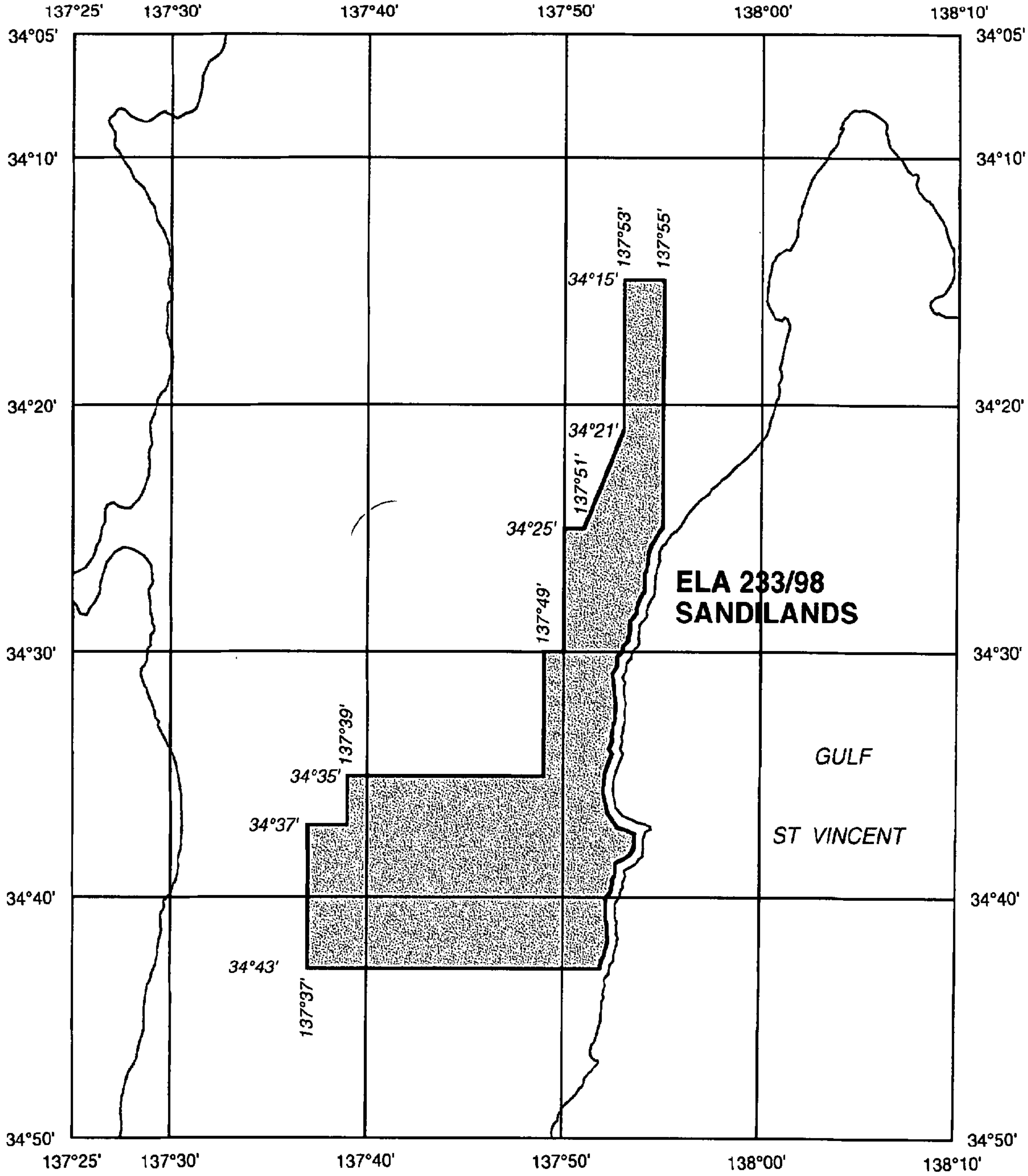

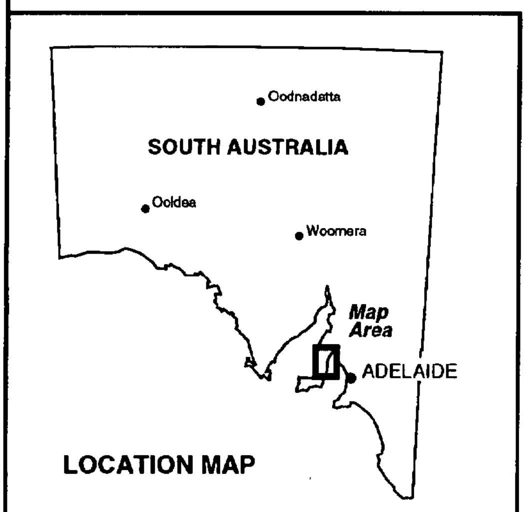

Scale 1 : 500,000

0 5 10 15 20 25 km

Transverse Mercator Projection. AMG Zone 53.

Microstation

Prepared : RRM	BHP Exploration - BHP Minerals BHP Minerals Pty. Ltd., A.C.N. 008 694 782	Centre : Brisbane
Drawn : RRM	ELA 233/98, SANDILANDS, SOUTH AUSTRALIA	A4-2307
Date : Nov 1998	**LOCATION MAP**	**FIGURE 1**
Revised :		

4. WORK COMPLETED

4.1 GEOTEM Survey

The Moonta GEOTEM survey was flown by Geoterrex-Dighem Pty Ltd for BHPM during July-August 1998. An application was lodged immediately after the survey was flown (ELA 2578), in order to cover an anomaly identified in the southern part of the survey area.

All lines were oriented east-west at 500 m line spacing for a total of 2761 line km. Data were collected using the $GEOTEM_{DEEP}$ airborne electromagnetic and magnetic system, with a base operating frequency of 25 Hz, employing a multi component electromagnetic receiver (X, Y and Z components). Real time differential GPS was used for navigation.

The GEOTEM field data were processed to remove atmospheric and system noise using PC work stations and advanced GMAPS software. Algorithms were applied to create Amplitude Decay Index (ADI) and altitude corrected data sets for both X and Z components. A full logistic report is included in **Appendix 2** and a GEOTEM image is included on **Figure 2**.

The specifications of the GEOTEM III system and survey are shown below:

GEOTEM III	
Platform:	CASA 212-200
Tx Height:	105 m
Rx Height:	54 m
Tx – Rx Separation:	100 m
Tx pulse width:	4 ms
Tx off time:	16 ms
Waveform:	Half-sine wavepulse
FREQUENCY:	25 –125 Hz
Tx Moment:	710 000 Am^2
Rx coils:	x,y,z
Samples per waveform:	384
Measured:	dB/dt, B field
Line Spacing:	500 m

A geological interpretation of the southern survey area shows the area is dominated by quartzo-feldspathic rocks and granite. This interpretation is reinforced by the GEOTEM which shows the southern survey area to be particularly resistive (i.e. northern part of EL 2578). Cover sequences in this area are dominated by limestones which are less susceptible to weathering and form a resistive overburden.

GEOTEM interpretation consisted of line by line interpretation through GemeX and multiplots and image interpretation. Several anomalies were picked and ranked according to their GEOTEM response. One GEOTEM anomaly was recognised on EL 2578 and details are shown below.

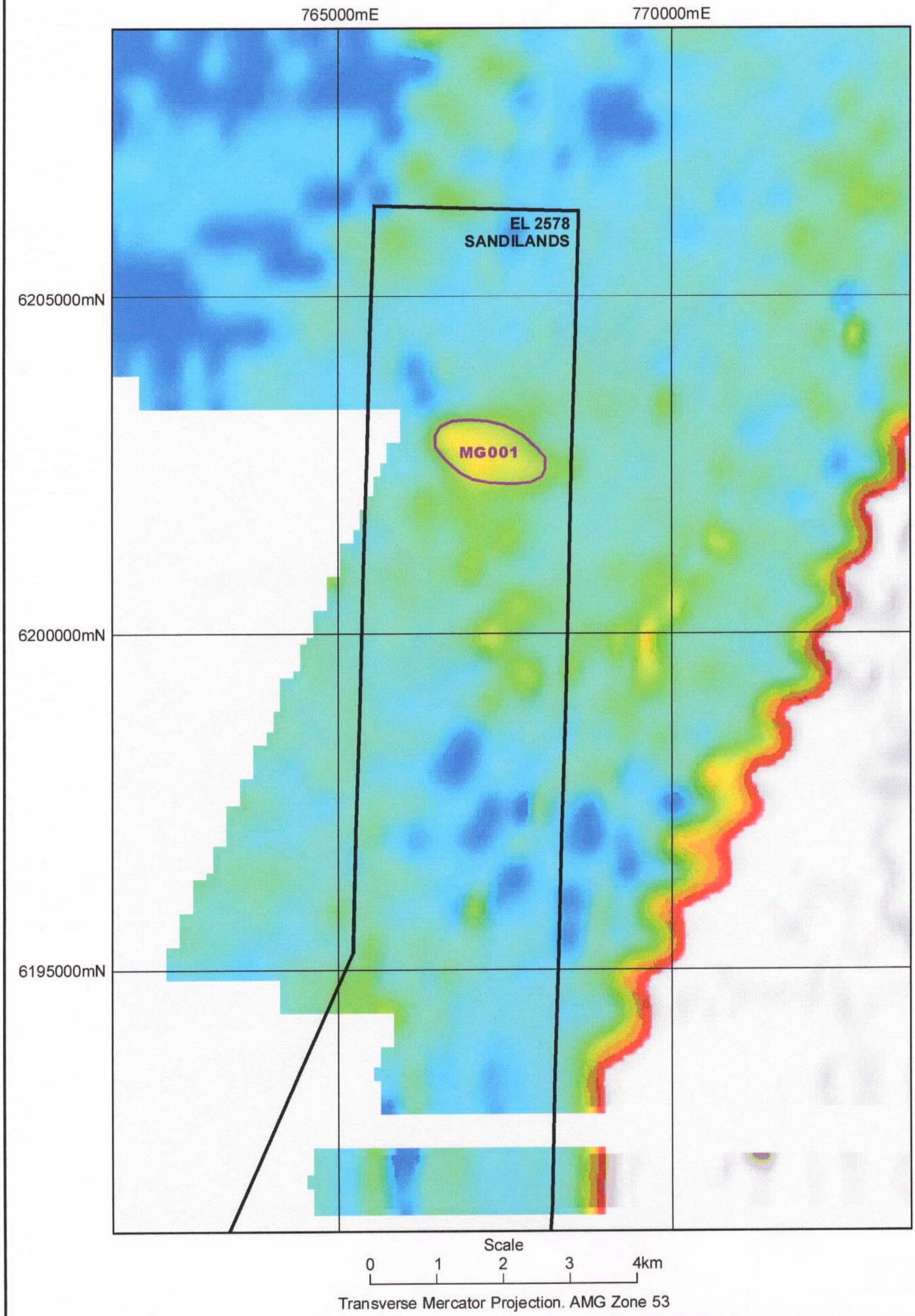

Prepared : M.Whittall	BHP — Minerals Discovery Group, BHP World Minerals, The Broken Hill Proprietary Company Limited A.C.N. 004 028 077	Centre : Brisbane
Drawn : C.J.W		Drawing No.: CDB1689
Date : April 2000	EL 2578 SANDILANDS, SOUTH AUSTRALIA	
Revised :	**GEOTEM IMAGE**	**FIGURE 2**

Anomaly #:	MG001
Priority:	moderate
Lines:	1891, 1901
East:	767519
North:	6202897
Taux:	15, 17 = 2.07 and 15, 17 = 2.36
Tauz:	16, 18 = 2.00
Approx Depth:	<50
Comments:	1 km wide with 2 peaks striking NE
Geology:	Probably sediments, limestone ?

Anomaly MG001 was downgraded and consequently was not followed up. No field work was carried out over the anomaly or any other part of the EL during the period.

6. CONCLUSIONS

EL 2578 was pegged in order to cover a GEOTEM anomaly from BHPM's Moonta survey flown in 1998, and the Curramulka magnetic complex further south. Exploration work by BHPM during the period consisted of an assessment of the GEOTEM anomaly MG001, and some magnetic targets further south. All anomalies were downgraded during this process, and consequently the tenement was surrendered after 12 months of being granted. No further work is recommended.

APPENDIX 1

EXPENDITURE REPORT

Exploration Expenditure Report

Tenement Name: Sandilands
Tenement Number: EL 2578
Tenement Grant Date: 27 January 1999
Tenement Expiry Date: 26 January 2000

	Selected Period	Life to Date
Wages and Salaries	2550	2,550
Vehicles		96
Geophysics		26,705
Field Running Costs	16	16
Consultants/Contractors	718	718
Admin & Office Overheads (10%)	328	3,009
TOTAL EXPENDITURE	**$3,612**	**$33,094**

APPENDIX 2

LOGISTICS REPORT FOR THE GEOTEM SURVEY

LOGISTICS REPORT

FOR A GEOTEM$_{DEEP}$® AIRBORNE ELECTROMAGNETIC AND MAGNETIC SURVEY FOR BHP MINERALS EXPLORATION PTY. LTD.

MOONTA SURVEY AREA, SOUTH AUSTRALIA

October 1998

Compiled by :
Brett Lantzke

GEOTERREX-DIGHEM PTY LIMITED
7-9 GEORGE PLACE ARTARMON, (SYDNEY), N.S.W 2064

geoterrex-dighem

Airborne & Ground Geophysics

TABLE OF CONTENTS

FIGURES

TABLES

1. INTRODUCTION

A **$GEOTEM_{DEEP}$®** airborne electromagnetic / magnetic survey was flown by Geoterrex-Dighem Pty Limited for BHP Minerals Exploration PTY. LTD. from the 30th July to the 5th August 1998. The survey area is located near Port Perie, South Australia and can be located on the 1:250,000 Australian Map Sheet : SI 53-08 "Whyalla" / SI 53-12 "Maitland" / SI54-09 "Adelaide". The survey coverage consisted of 2,761 line kilometres, flown in 7 flights. No tie lines were flown for the area. The details of the survey area are provided in **Table 1**.

The survey employed the **$GEOTEM_{DEEP}$®** electromagnetic system, operating at a base frequency of 25Hz. Ancillary equipment consisted of a magnetometer, radar altimeter, video camera, analogue and digital recorders and an electronic navigation system. The instrumentation was installed in a CASA C212-200 Turbo Prop survey aircraft. The aircraft was flown at an average speed of 235km/h with an average EM bird receiver height of 62m.

Table 1: The Moonta Survey Area

Area	Base of Operations	Line Spacing (m)	Line Direction
Moonta	Port Pirie	500	090°-270°

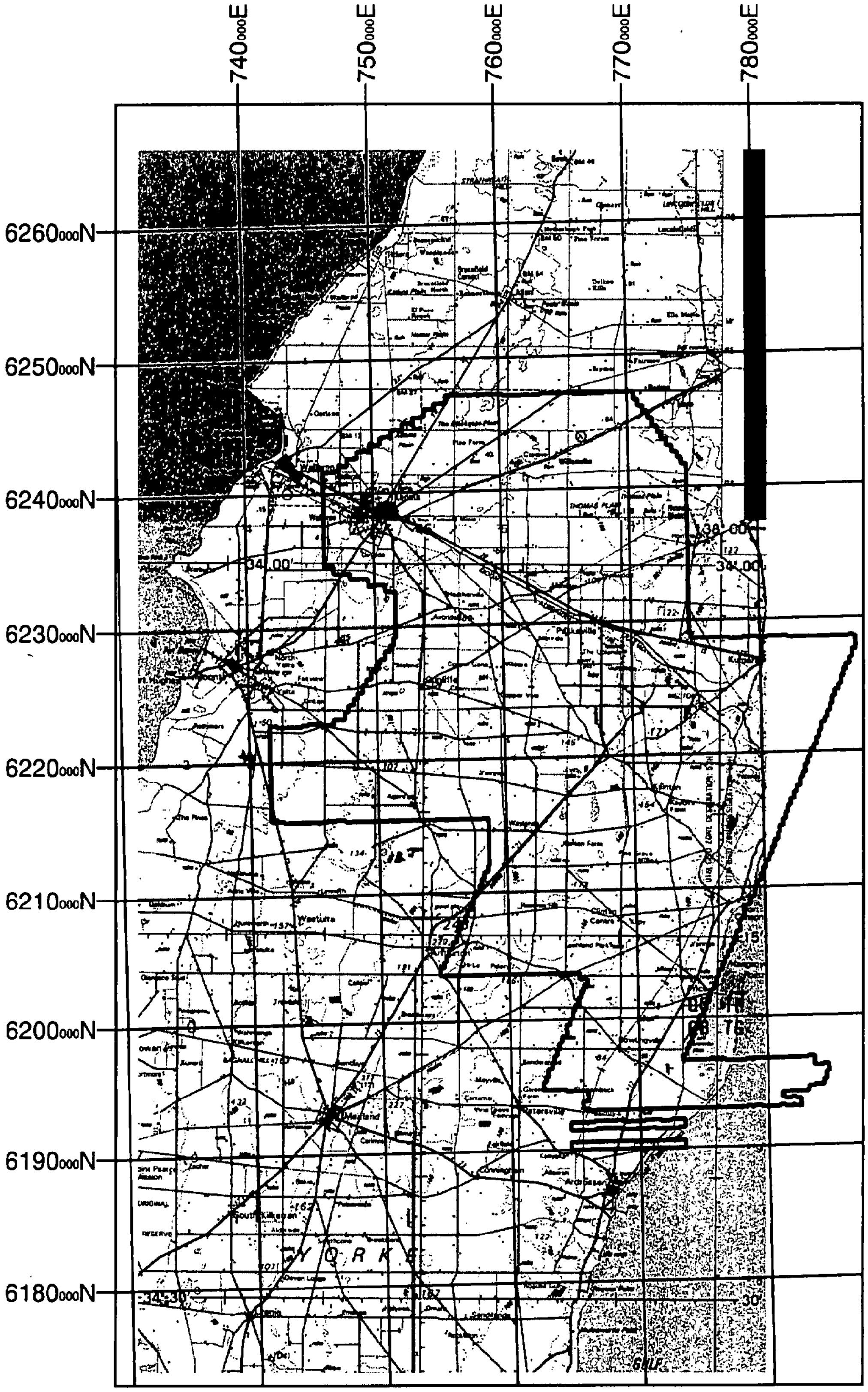

Figure 1: Location map: Moonta Survey Area, South Australia.

Figure 1: Location Map: Moonta Survey Area, South Australia. (Also see previous page)
Scale: 1:250,000

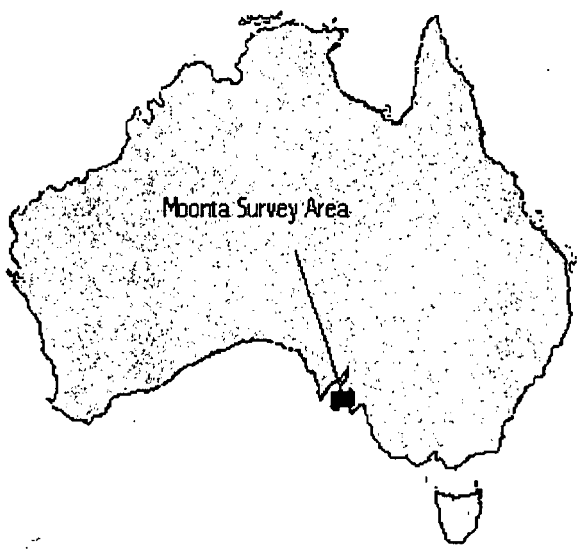

2. SURVEY OPERATIONS SUMMARY

During the course of the survey, weekly production reports were produced by the crew manager to outline the surveys progress. A summary has been produced from these reports to give an outline of the Survey's progression (**Table 2**), as well as the personnel involved in the survey (**Table 3**).

Table 2: Survey Progress

Date	Progress
July 1998	
30	Mobilization to site, Port Pirie
31	Survey commenced, flights 1.
August 1998	
1	Flight 2 . Half day pilot testing.
2	Flight 3 & 4
3	Flights 5
4	Flights 6
5	Flight 7, survey completed. Demobilization from site.

Table 3: Survey Personnel

Position	Crew Member
Crew Manager	A. Cole
Pilots	McGuire, Harradance, Kaloty, Haldane
Aircraft Engineer	G. Pullen
Electronics Technicians	A. Cole
Geophysicists / Processors	S. Jagar, R. Costelloe

3. SURVEY EQUIPMENT

In the acquisition of airborne geophysical data, there are many different parameters associated with the equipment used in the survey. Some of these specification have been outlined in **Table 4**. **Figure 2** gives a diagrammatical representation of the configuration of the airborne electromagnetic system .

Table 4: Airborne Equipment Specifications

System Parameters		**GEOTEM$_{DEEP}$®** Specifications
Navigation		Real time Differential GPS
Nominal aircraft speed (m/s)		65
Geometry	Transmitter height above ground level (m agl) (Nominal terrain clearance)	105
	Receiver Bird Height (agl, m)	63
	Tx-Rx horizontal separation (m)	114
Transmitter	Coil Axis	Vertical
	Signal	Half sine wave current pulse
	Base frequency (Hz)	25
	Repetition rate (pulses per second)	40
	Pulse width (microseconds)	4108
	Loop area (square metres)	231
	Number of turns	6
	Peak Current (amps)	≈ 480
	Tx loop dipole moment (Am^2)	6.65×10^5
Receiver	Coil Axes	X, Y and Z
	Sample Interval (seconds)	0.25
	Channel times	see Table 5

Figure 2: GEOTEM$_{DEEP}$® System Geometry

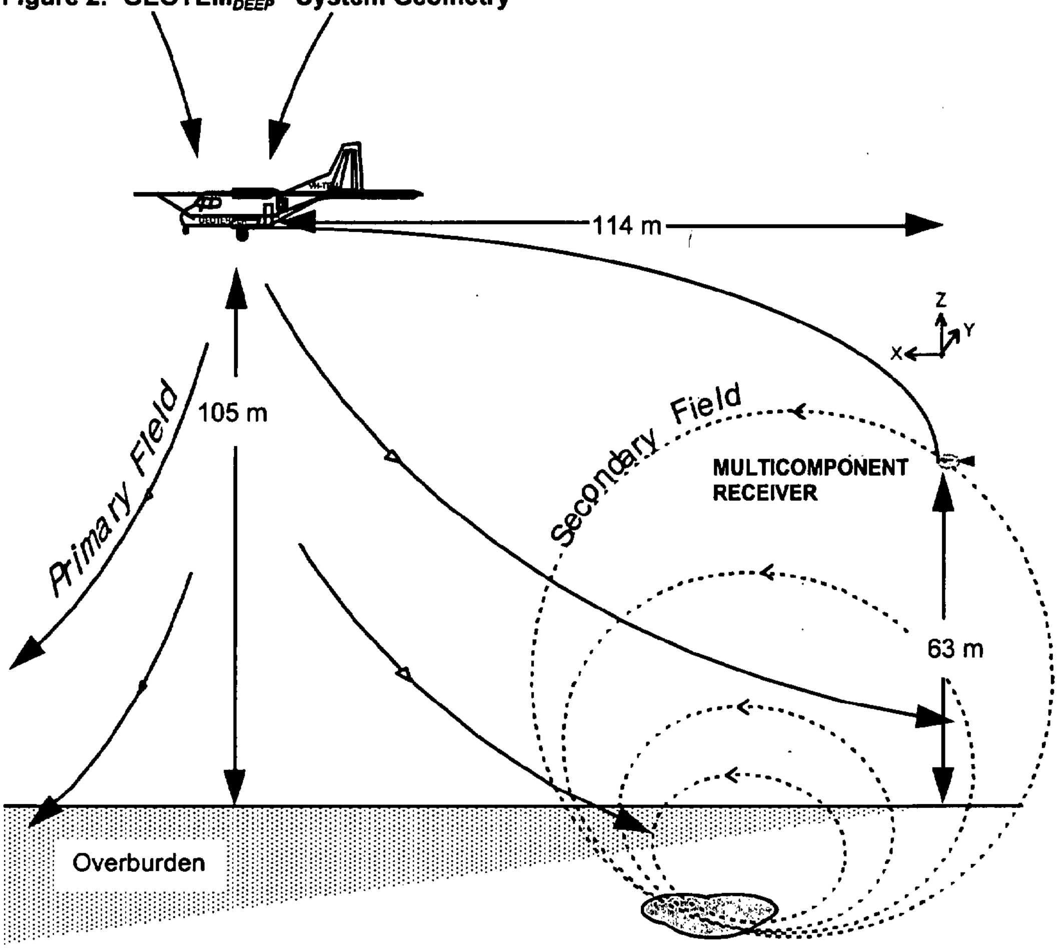

The wave form that is used by **GEOTEM$_{DEEP}$®** is a half rectified sine wave pulse, which alternates polarity. This can be seen in Figure 3 with respect to the current. Once the **GEOTEM$_{DEEP}$®** is transmitting the alternating pulse, a primary field is produced (V_P) which it turn produces a secondary field (V_S). These two fields combine to produce the Total field (V_T) which is measured by the receiver (Figure 3).

Figure 3: The characteristics of the Transmitted, Primary and secondary wave forms.

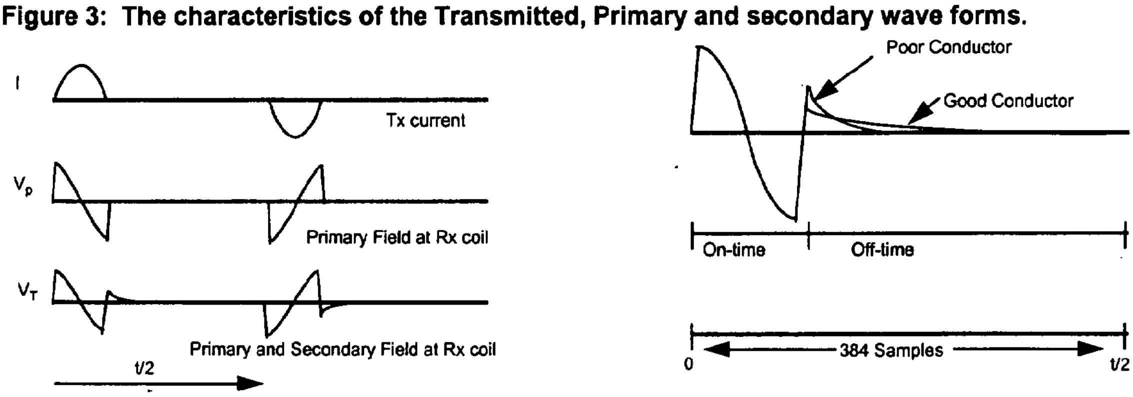

To measure the total field (V_T), a set of 20 channels are set up in which the receiver reads. These channels, or windows, are positioned so that there are 4 channels in the on time of the pulse and 16 channels in the off time. The centre of each window , with respect to the end of the pulse, are recorded in **Table 5**.

Table 5: Receiver Channel Positions

Channel	Channel Centre usec after Tx off	Channel Width usec
1	-3866	469
2	-3085	1094
3	-1913	1250
4	-507	1563
5	352	156
6	509	156
7	665	156
8	899	313
9	1212	313
10	1602	469
11	2071	469
12	2618	625
13	3321	781
14	4181	938
15	5196	1094
16	6368	1250
17	7774	1563
18	9493	1875
19	11681	2500
20	14337	2813

To help visualise the correlation between the channel times and the electromagnetic (em) waves (the transmitted wave and the Total field), the channels have been superimposed on the em waves in Figure 4. A second Y axis scale has been placed on the diagram to show the em waves at a smaller scale, so that the finer detail in the later channels can be seen. The data for these later channel is represented by the dashed lines.

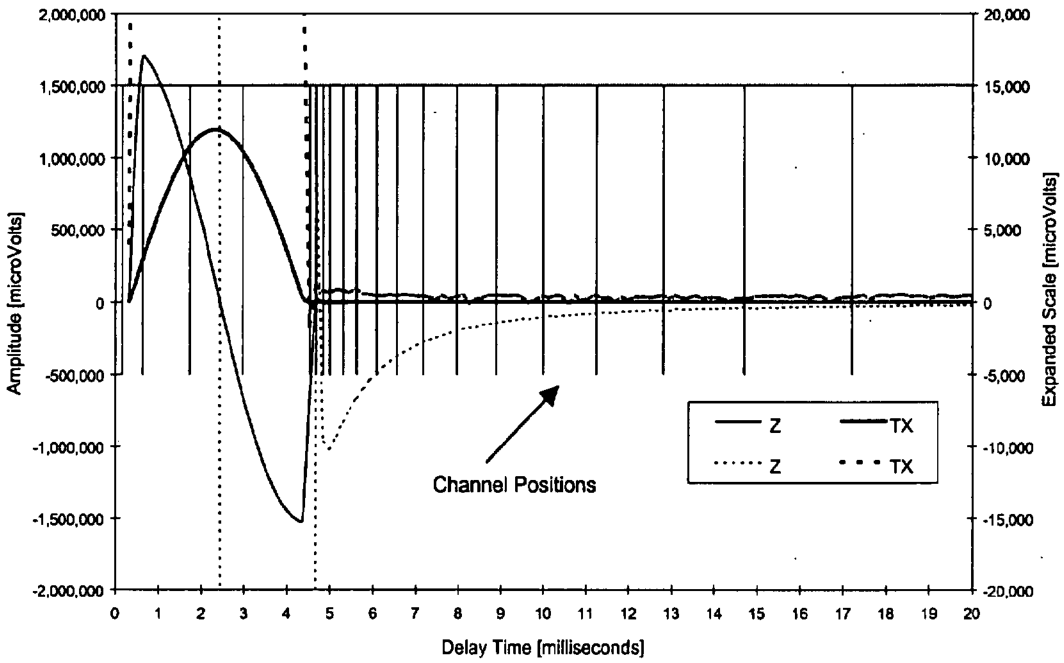

Figure 4: The transmitted pulse and the received Z component overlayed by the channel times.

3.1 Electromagnetic Acquisition System

For the acquisition and recording of the data for the **GEOTEM$_{DEEP}$®**, a purpose built GEODAS logging and processing system is used. The GEODAS is a computer-based software system using a Pentium field PC. It runs multiple DOS programs in a multi-tasking environment. The modular design of the GEODAS allows for re-configuration of the system to record different types of surveys by adding, removing, or changing task modules.

Model:	Geoterrex-Dighem Pty Limited GEODAS
Equipment:	Pentium PC
Recording Mode:	Hard disk transferred to Jazz disk

The GEODAS is installed on a rugged, totally enclosed, moisture and dust-proof system, originally designed for military use. Currently, the GEODAS uses a Pentium CPU on a plug-in module card that can be upgraded.

The following are recorded digitally using the GEODAS:

Each second:	Flight number Navigation data Total magnetic field Fiducial number (time in seconds) Altitude (radar and barometer)
Each 0.25 secs:	20 X, Y, & Z component dB/dt **GEOTEM$_{DEEP}$®** channels 20 X, Y, & Z component B-field **GEOTEM$_{DEEP}$®** channels X, Y, & Z component transmitter primary field Power line noise monitor (X, Y, & Z component) Earth field monitor (X, Y, & Z component) Earth field correction

3.2 Magnetometers

There were two types of magnetometers used in survey. The survey magnetometer, which is an optically pumped Cesium vapour magnetometer, and the base station, which is a proton procession magnetometer. There respective specifications are set out below.

3.2.1 Survey Magnetometer

Model:	Cesium vapour optical absorption magnetometer sensor
Mounting:	Tail stinger
Sample period:	50 milliseconds
Sample interval:	1.0 seconds *
Sensitivity:	0.01 nanoTeslas (nT)
Recording:	Digital data is sent to a Jazz drive and also displayed on aircraft chart recorder

* To operate both the **GEOTEM$_{DEEP}$®** system and the magnetometer system simultaneously, the transmitter is switched off for a period of 200 milliseconds every second to allow for a noise free magnetometer reading

3.2.2 Base Station Magnetometer

The base station magnetometer operates during flying hours to monitor the diurnal variations in the magnetic field. The sensor is placed in a suitable position that minimises the effects of high magnetic gradients and cultural interference. A second base station is operated as a back-up.

Model:	G856 Proton Precession magnetometer
Sample interval:	5 seconds
Sensitivity:	0.1 nanoTeslas (nT)
Recording:	Internal memory(backed up daily)

3.3 Tracking Camera

The tracking camera is equipped with a 4 mm wide-angle lens. The video tape is synchronised with the geophysical record by a digital fiducial display that is recorded on the video tape. This digital display of the fiducial mark can be found on the bottom left hand corner on each frame of the video. Times are recorded from the digital information provided by the data acquisition system. The video is recorded in PAL format.

Model:	Sony DXP 101P Camera with wide angle lens
	Panasonic AG6400 Video Cassette Recorder
	Sony PVM 6030ME Monitor

3.4 Altimeters

To establish the height of the aircraft above the ground, two altimeters are used, barometric and radar. Both the two different altimeters are used to compliment each other so that the plane can kept a constant drape flying height. The specifications of the altimeters can be found below.

3.4.1 Barometric Altimeter

The barometric altimeter is plotted on the aircraft chart recorder during the flight and is also recorded onto the Jazz drive as digital data.

Model:	Geoterrex-Dighem Barometric Transducer (SENSYM 142SC15A)
Sample interval:	1.0 seconds
Sensitivity:	0.24 mV/foot (6.5 mV/mb)

3.4.2 Radar Altimeter

The Sperry radio altimeter is a high quality instrument whose output is factory calibrated. It is fitted with a test function which checks the calibration of a terrain clearance of 100 feet and altitudes which are multiples of 100 feet. The aircraft radio altitude is recorded onto a Jazz drive, as well as being displayed on the aircraft chart recorder. The recorded value is the average of the altimeters output during the previous second.

Model:	Sperry Stars AA200 radio altimeter system
Sample interval:	1.0 second
Accuracy:	+/- 1.5% of indicated altitude.

3.5 Electronic Navigation

GPS equipment:	Sercel NR103 GPS receiver and antennae mounted in aircraft and equipped with steering indicators.
Base station:	Sercel NR103 & Ashtech GG24 GPS receivers with lap-top.
Sample rate:	0.6 seconds
Differential corrections:	OMNISTAR – Fugro by Starfix
Doppler equipment:	Singer Kearfott AN/ASN 128, Sperry VG-14 Vertical Gyroscope, Sperry C-12 Compass.
Sample rate:	1.0 seconds

The Global Positioning System (GPS) is a line of sight, satellite navigation system that utilises time-coded signals from at least four of the twenty-four NAVSTAR satellites. In the differential mode, two GPS receivers are used. An OMNISTAR system receives GPS differential corrections and transmits these to the acquisition GPS on board the aircraft. These corrections are applied to the raw GPS data in real time for navigation. From this corrected data the on-board system calculates the flight path of the aircraft. This system gives a post-survey processing accuracy of approximately 5 metres,

The GPS records data relative to the WGS84 ellipsoid, which is the basis of the revised North American Datum (NAD83). Conversion software is used to transform the WGS84 coordinates to Australian Map Grid (AMG) coordinates using the AGD66 datum.

3.6 Analogue Recorder

The analog recorder is a thermal dot matrix printer that records selected channels to aid in the quality control of the data that is being acquired. Below, a list of the selected channels is given.

Model:	RMS GR33 Thermal Dot Matrix Printer
Chart speed:	11 cm/minute; time increases from left to right
Chart width:	31 cm
Event marks:	20 second marks are recorded on the bottom of the chart with the associated fiducial numbers being printed at the base of the chart.
GEOTEM$_{DEEP}$® Traces:	The scales for the **GEOTEM$_{DEEP}$**® traces are displayed on the analogue charts. The zero line for each channel is separated by 0.5 cm with the latest channel always being plotted closest to the bottom of the page.
Synchronisation:	A lag of approximately 5.0 seconds occurs between the **GEOTEM$_{DEEP}$**® channels and the magnetometer and altimeter traces.
Channels Displayed:	Primary field monitor (X, Y and Z) Earth field monitors (X, Y and Z) Total magnetic field - fine and coarse scale Terrain clearance - radar Barometer Selected **GEOTEM$_{DEEP}$**® X and Z dB/dt channels (Channels 6, 13 and 20) Selected **GEOTEM$_{DEEP}$**® X and Z B field channels (Channels 6, 13 and 20) Powerline monitor X component dB/dt noise trace (X_n1) X component B field noise trace (X_n2)

As the thermal paper used in the analog recorder tends have problems under certain conditions. The final chapter has information regarding the best conditions for the plots to be stored.

Figure 5: Analogue Chart Sample

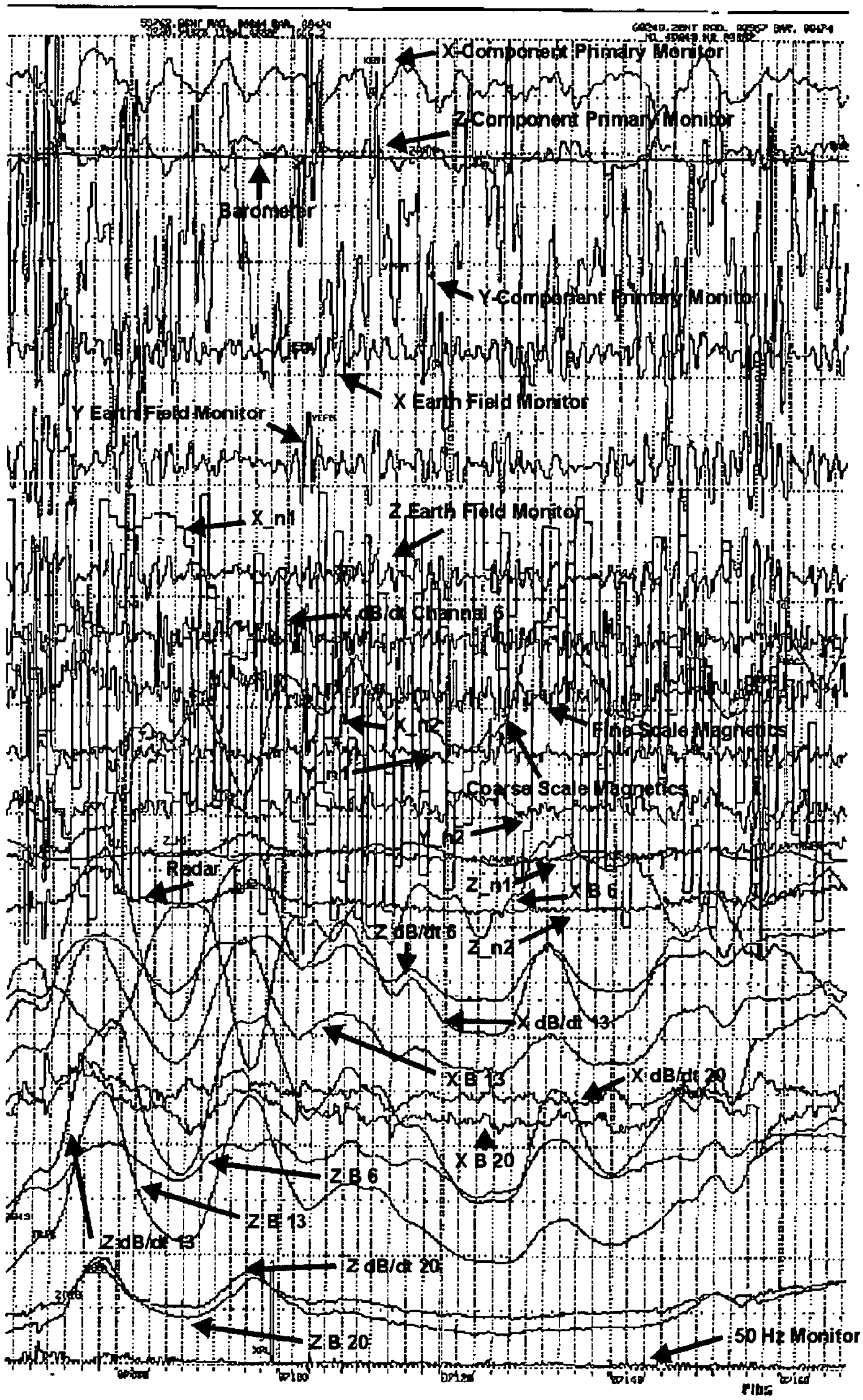

3.7 Equipment Tests and Calibrations

3.7.1 Electromagnetic Lag Test

An electromagnetic lag test is routinely carried out to determine the lag of the **GEOTEM$_{DEEP}$®** system. The test is conducted by flying in two different directions over a known target with a particular electromagnetic signature. The response of the target is plotted as a stacked profile (Figure 6). The value calculated by the electromagnetic test is used in the processing of the **GEOTEM$_{DEEP}$®** electromagnetic data. For this survey, the results of a previous electromagnetic lag test flown in Nyngan, New South Wales, were used in the processing of the electromagnetic data.

Figure 6: Example of an Electromagnetic Lag Test

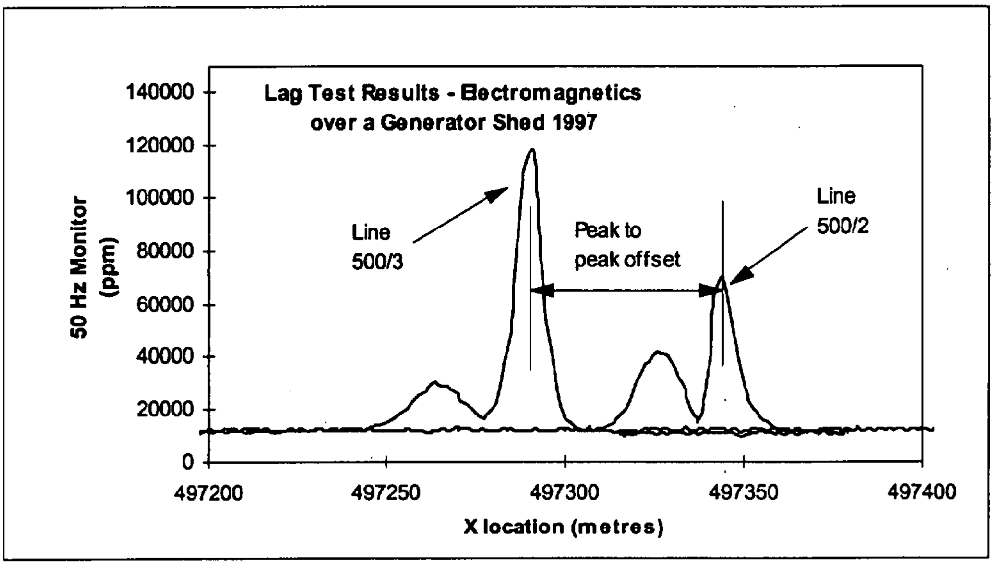

3.7.2 Figure of Merit Test

The figure of merit test is routinely carried out to determine the noise induced in the magnetometer resulting from rolls, pitches and yaws. The test is carried out at a high altitude over an area of low magnetic gradient. The aircraft carries out +/- 10° rolls, +/- 5° pitches and +/- 5° yaws over periods of 4-5 seconds in the same direction as the flight lines. For this survey, the results of a previous figure of merit test flown in Nyngan, New South Wales were used in the processing of the magnetic data.

3.7.3 Cloverleaf Test

The cloverleaf test is flown to determine the effect of the sensor heading and orientation on the magnetic sensors reading, relative to the direction of the earth's magnetic field. The magnetic heading effect is determined by flying a cloverleaf pattern oriented in the same directions as the survey lines. At least two passes in each direction were flown over a recognisable feature on the ground in order to obtain sufficient statistical information to estimate the heading error. For this survey, the results of a previous cloverleaf test flown in Nyngan, New South Wales were used in the processing of the magnetic data.

3.7.4 Magnetometer Lag Test

The aircraft was flown in opposite directions over a sharp magnetic anomaly with the navigation system and magnetometer operating. Positioning of the magnetic high is determined from the navigation system for each line direction. The numerical difference in the position of the two peaks is the 2-way or total lag (Figure 6). This total lag is halved to find the one-way lag which is used to correct the magnetic data. The changes in lag due to varying ground speed are compensated for in the processing. For this survey, the results of a previous magnetometer lag test flown in Nyngan, New South Wales were used in the processing of the magnetic data.

Figure 7: Example of a Magnetic Lag test

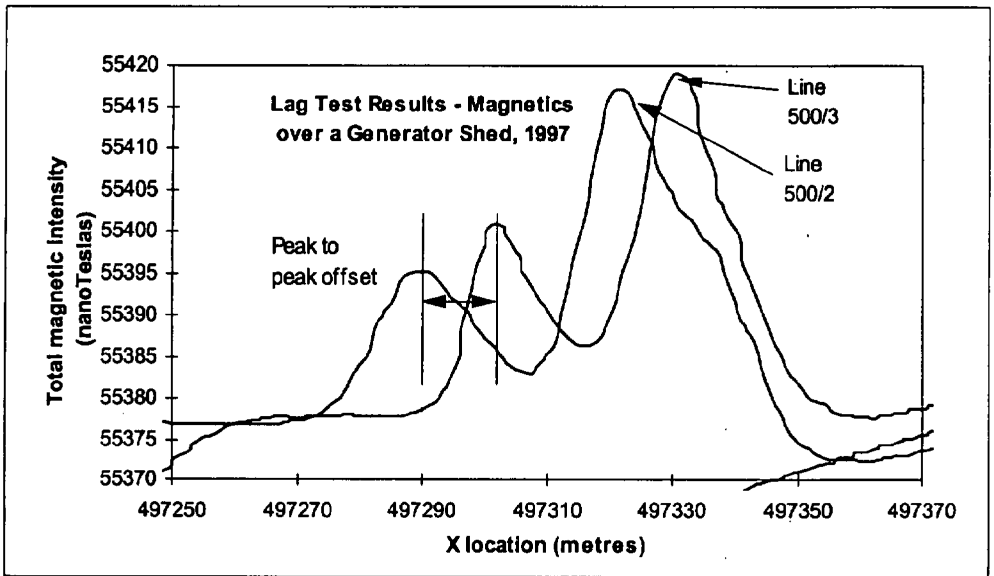

3.8 GPS Positioning tests

A position accuracy test of the real time satellite DGPS - OMNISTAR navigation system and the Sercel post-processed GPS positioning system was carried out prior to the beginning of the survey.

The aircraft, which uses the OMNISTAR system is positioned so that the GPS sensor is located at a known point. Positional data is then recorded and check for accuracy by comparing the data to the known location..

The Sercel GPS base station was located by placing the mobile Sercel unit on a known trig location and monitoring the movement of the base station at the field processing office (hotel). The position of the field processing office base station GPS was averaged for data recorded over two hours. The Z component of the positioning test can also be used to compare against the radar and barometric altimeter data. For this survey, the results of a previous GPS Positioning test performed in Nyngan, New South Wales were used.

4. PRODUCTS AND PROCESSING

4.1 Field Processing

Raw **GEOTEM$_{DEEP}$®** data collected in the field on a Jazz drive and is read directly onto a Pentium PC, where advanced Windows NT GMAPS processing software is applied to the data. In this way, an improved delivery schedule for final processed data is achieved.

Processed data is displayed as profiles and plans in the field. Displays are produced of flight path plots, magnetic and ADI images, and EM channel amplitudes. Geoterrex-Dighem Pty Limited uses these displays to analyse the quality of the data collected.

The field processing centre also includes another Pentium PC for additional tasks such as down loading base station data.

Field Processing System

Hardware:	Lap-top Pentium PC's operating on a Windows NT platform Jazz drive Encad A1 plotter HP Printer
Software:	Geoterrex-Dighem Pty Limited developed GMAPS **GEOTEM$_{DEEP}$®** processing software ER Mapper Image processing software

Office Processing System

Hardware:	Pentium PC network and peripherals operating on a Windows NT platform Exabyte, DAT, CD-ROM, and Jazz data transport devices High speed HP Printers HP 750C Designjet Plotters Cartographic Workstation
Software:	Geoterrex-Dighem Pty Limited developed GMAPS **GEOTEM$_{DEEP}$®** processing software Geoterrex-Dighem Pty Limited developed VISION image processing software ER Mapper image processing software

4.2 Electromagnetics

There are many steps in the processing of the airborne and they are broken down into the following.

4.2.1 Levelling

Since the **GEOTEM$_{DEEP}$®** receiver constantly normalises and calibrates during data acquisition there is no levelling of data at the post-survey processing stage.

4.2.2 Synchronisation Lag

All **GEOTEM$_{DEEP}$®** and auxiliary geophysical data have been synchronised with navigation data so that there is no "peak position" offset between the responses obtained from lines flown in opposite directions over a narrow vertical conductor. See 3.7.1.

4.2.3 Noise Reduction

Noise reduction in the digital data is accomplished by identification of the noise type (atmospheric, system or cultural), analysis of the spectral content of the entire signal (geological + noise) and selective filtering.

4.2.3.1 Atmospheric Noise

The first stage of processing is atmospheric (spheric) noise removal which is achieved by using a method based loosely on cross correlation and non linear filtering. These filters are used since most spheric events are single point spikes, impulse responses, and linear filtering is not effective at properly removing the noise without having an effect on the surrounding data.

4.2.3.2 Cultural noise

Cultural noise (which includes sources such as 50 Hz powerlines, electric fences, cathodic protected metal structures) is measured by the 50 Hz monitor. Normally cultural noise is not removed during processing.

4.2.3.3 System noise

System noise is removed by filtering using strict amplitude and wavelength thresholds to correctly isolate noise from geological signal. The filter shape and amplitude thresholds are determined on a flight by flight basis from raw data plots of at least 2 flight lines flown in opposite directions at the beginning and end of the flight. This allows customised filtering for directional, diurnal and flight noise, ensuring that the minimal amount of filtering is performed so that real signal is not degraded by using a "lowest common denominator" philosophy of applying one filter (usually the maximum) for all noise conditions.

4.2.4 Amplitude-weighted Decay Index (ADI)

To aid interpretation of the data, time constants can be calculated to quantify the rate of decay of the electromagnetic response. The Amplitude Decay Index (ADI) measures the rate of decay and weights it for the relative amplitude of the electromagnetic response. In this respect, the Amplitude Decay Index is also a measurement of the area under the decay curve rather than just an estimate of the rate of decay. The index is derived from the best fitting exponential to the decay curve using data from selected **GEOTEM$_{DEEP}$®** channels (minimum of four) as indicated on the profiles and this index is included on the final located data tape.

4.2.5 Altitude Correction

Altitude corrected **GEOTEM$_{DEEP}$®** data is presented on the multi-plots as faint lines along the same axis, base lines and scaling used for final processed channels. This presentation serves to highlight those areas where the electromagnetic response has been affected by variation in aircraft terrain clearance. This aids data interpretation by correcting the data to the mean survey altitude. Unexpectedly large variations in altitude are not corrected so as to avoid drastic distortion of the **GEOTEM$_{DEEP}$®** data.

4.3 Magnetics

The magnetic data is collected on two levels, the airborne magnetometer and the base station ground magnetometer. Once both sets of data have been check for spikes (spherical noise), further processing occurs in the following order.

4.3.1 Diurnal Levelling

Base station data is edited so that all significant spikes, level shifts and null data are eliminated. The data is re-sampled and synchronised to the airborne fiducial system prior to subtraction from airborne magnetic readings.

4.3.2 Synchronisation Lag

A lag was applied to synchronise the magnetic data with the navigation data.

4.3.3 IGRF Removal

The International Geomagnetic Reference Field (IGRF) 1995 model (updated for secular variation) was removed from the levelled total field magnetics. Finally an arbitrary datum of 2000 nT was added back.

4.4 Flight Path Recovery

A GPS receiver mounted in the survey aircraft uses 3D triangulation of satellite signals to calculate both the position of the aircraft in real time and to provide pilots with steering information. GPS data is read into the field computer and plotted on a daily basis to control data quality and determine any re-flights. Positioning data is stored digitally in WGS84 spheroid and later converted to Australian Map Grid (AMG) coordinates using the AGD66 datum. Raw GPS data is corrected real time with differential corrections transmitted via satellite, improving the accuracy of the position data recorded.

The integrated aircraft track is plotted on a daily basis. Plots are analysed to ensure data quality and to determine any re-flights.

4.5 Survey Products

4.5.1 Multi-Parameter Profile Plots

Final **GEOTEM$_{DEEP}$®** data (and the altitude corrected **GEOTEM$_{DEEP}$®** data) are presented as multi-parameter profiles after final processing in the Geoterrex-Dighem office in Sydney. The processed geophysical data is plotted at suitable scales from top to bottom, as listed in **Table 6** and **Table 7**. Altitude corrected data is plotted as faint lines with the processed data The x-axes of alternate sections of each plot are annotated with fiducial numbers or AMGs. The scales for the **GEOTEM$_{DEEP}$®** traces vary according to the channel, to allow resolution in late channels whilst keeping early channels on scale. The base level for each channel is separated by 0.5 cm with the latest channel always being plotted closest to the bottom of the page. Each plot has a title containing line number, job number, area name, frequency, pulse width and average northing or easting.

Table 6: Multi-Parameter Profile Plot Scales 1:25,000 horizontal scale for Final B field.

Panel	Channel	Trace Colour	Scale
1 (top)	Residual Magnetics Coarse Scale	Red	250 nT/cm
	Residual Magnetics Fine Scale	Green	100 nT/cm
	Barometric Altimeter	Black	20m/cm
	Radar Altimeter	Blue	20m/cm
2	Final B field		
	Z Offtime Channels 5-8	Black	160 pT/cm
	Z Offtime Channels 9-12	Blue	140 pT/cm
	Z Offtime Channels 13-16	Green	120 pT/cm
	Z Offtime Channels 17-20	Red	100 pT/cm
	50 Hz Monitor - Z Component	Black	160 microvolts/cm
3	Final B field		
	X Offtime Channels 5-8	Black	160 pT/cm
	X Offtime Channels 9-12	Blue	140 pT/cm
	X Offtime Channels 13-16	Green	120 pT/cm
	X Offtime Channels 17-20	Red	100 pT/cm
	50 Hz Monitor - X Component	Black	160 microvolts/cm

Table 7: Multi-Parameter Profile Plot Scales 1:25,000 horizontal scale for dB/dt.

Panel	Channel	Trace Colour	Scale
1 (top)	Residual Magnetics Coarse Scale	Red	200 nT/cm
	Residual Magnetics Fine Scale	Green	100 nT/cm
	Barometric Altimeter	Black	20m/cm
	Radar Altimeter	Blue	20m/cm
2	dB/dt		
	Z Offtime Channels 5-8	Black	50 nT/s/cm
	Z Offtime Channels 9-12	Blue	40 nT/s/cm
	Z Offtime Channels 13-16	Green	30 nT/s/cm
	Z Offtime Channels 17-20	Red	20 nT/s/cm
	50 Hz Monitor - Z Component	Black	50 microvolts/cm
3	dB/dt		
	X Offtime Channels 5-8	Black	50 nT/s/cm
	X Offtime Channels 9-12	Blue	40 nT/s/cm
	X Offtime Channels 13-16	Green	30 nT/s/cm
	X Offtime Channels 17-20	Red	20 nT/s/cm
	50 Hz Monitor - X Component	Black	50 microvolts/cm

4.5.2 Flight Path Maps

Flight path maps were produced on film at 1:50,000 scale. These were annotated with line numbers, flight direction and fiducial position.

4.5.3 Data Media And Format

A set of located data files were produced and written CD ROM. The data layout within these files is given in the following tables.

4.5.4 Items Delivered

1. Final Maps @ 1:50,000

Flight path maps (black line on film)
Multi-parameter profile plots @ 1:50,000

2. Digital Products

Located data on CD ROM and associated documentation

3. Additional Products

Analogue chart records
Logistics report
Flight path video cassettes
Flight logs
Mileage list
Final flight line list

Table 8: Located Data Tape Format – X, Y & Z GEOTEM$_{deep}$ Processed Data

Column Range		Field	Description
1	4	1	Flight number
5	10	2	Line identifier
11	19	3	Fiducial – seconds
20	29	4	Date (ddmmyy)
30	38	5	AMG Easting [ADG66] metres
39	48	6	AMG Northing [ADG66] metres
49	59	7	Latitude [ADG66]
60	71	8	Longitude [ADG66]
72	81	9	X GEOTEM$_{deep}$ Inpulse Channel 1 Processed nT/s
82	91	10	X GEOTEM$_{deep}$ Inpulse Channel 2 Processed nT/s
92	101	11	X GEOTEM$_{deep}$ Inpulse Channel 3 Processed nT/s
102	111	12	X GEOTEM$_{deep}$ Inpulse Channel 4 Processed nT/s
112	121	13	X GEOTEM$_{deep}$ Channel 5 Processed nT/s
122	131	14	X GEOTEM$_{deep}$ Channel 6 Processed nT/s
132	141	15	X GEOTEM$_{deep}$ Channel 7 Processed nT/s
142	151	16	X GEOTEM$_{deep}$ Channel 8 Processed nT/s
152	161	17	X GEOTEM$_{deep}$ Channel 9 Processed nT/s
162	171	18	X GEOTEM$_{deep}$ Channel 10 Processed nT/s
172	181	19	X GEOTEM$_{deep}$ Channel 11 Processed nT/s
182	191	20	X GEOTEM$_{deep}$ Channel 12 Processed nT/s
192	201	21	X GEOTEM$_{deep}$ Channel 13 Processed nT/s
202	211	22	X GEOTEM$_{deep}$ Channel 14 Processed nT/s
212	221	23	X GEOTEM$_{deep}$ Channel 15 Processed nT/s
222	231	24	X GEOTEM$_{deep}$ Channel 16 Processed nT/s
232	241	25	X GEOTEM$_{deep}$ Channel 17 Processed nT/s
242	251	26	X GEOTEM$_{deep}$ Channel 18 Processed nT/s
252	261	27	X GEOTEM$_{deep}$ Channel 19 Processed nT/s
262	271	28	X GEOTEM$_{deep}$ Channel 20 Processed nT/s
272	281	29	Y GEOTEM$_{deep}$ Inpulse Channel 1 Processed nT/s
282	291	30	Y GEOTEM$_{deep}$ Inpulse Channel 2 Processed nT/s
292	301	31	Y GEOTEM$_{deep}$ Inpulse Channel 3 Processed nT/s
302	311	32	Y GEOTEM$_{deep}$ Inpulse Channel 4 Processed nT/s
312	321	33	Y GEOTEM$_{deep}$ Channel 5 Processed nT/s
322	331	34	Y GEOTEM$_{deep}$ Channel 6 Processed nT/s
332	341	35	Y GEOTEM$_{deep}$ Channel 7 Processed nT/s
342	351	36	Y GEOTEM$_{deep}$ Channel 8 Processed nT/s
352	361	37	Y GEOTEM$_{deep}$ Channel 9 Processed nT/s
362	371	38	Y GEOTEM$_{deep}$ Channel 10 Processed nT/s
372	381	39	Y GEOTEM$_{deep}$ Channel 11 Processed nT/s
382	391	40	Y GEOTEM$_{deep}$ Channel 12 Processed nT/s
392	401	41	Y GEOTEM$_{deep}$ Channel 13 Processed nT/s
402	411	42	Y GEOTEM$_{deep}$ Channel 14 Processed nT/s
412	421	43	Y GEOTEM$_{deep}$ Channel 15 Processed nT/s
422	431	44	Y GEOTEM$_{deep}$ Channel 16 Processed nT/s
432	441	45	Y GEOTEM$_{deep}$ Channel 17 Processed nT/s

442	451	46	Y GEOTEM$_{deep}$ Channel 18 Processed nT/s
452	461	47	Y GEOTEM$_{deep}$ Channel 19 Processed nT/s
462	471	48	Y GEOTEM$_{deep}$ Channel 20 Processed nT/s
472	481	49	Z GEOTEM$_{deep}$ Inpulse Channel 1 Processed nT/s
482	491	50	Z GEOTEM$_{deep}$ Inpulse Channel 2 Processed nT/s
492	501	51	Z GEOTEM$_{deep}$ Inpulse Channel 3 Processed nT/s
502	511	52	Z GEOTEM$_{deep}$ Inpulse Channel 4 Processed nT/s
512	521	53	Z GEOTEM$_{deep}$ Channel 5 Processed nT/s
522	531	54	Z GEOTEM$_{deep}$ Channel 6 Processed nT/s
532	541	55	Z GEOTEM$_{deep}$ Channel 7 Processed nT/s
542	551	56	Z GEOTEM$_{deep}$ Channel 8 Processed nT/s
552	561	57	Z GEOTEM$_{deep}$ Channel 9 Processed nT/s
562	571	58	Z GEOTEM$_{deep}$ Channel 10 Processed nT/s
572	581	59	Z GEOTEM$_{deep}$ Channel 11 Processed nT/s
582	591	60	Z GEOTEM$_{deep}$ Channel 12 Processed nT/s
592	601	61	Z GEOTEM$_{deep}$ Channel 13 Processed nT/s
602	611	62	Z GEOTEM$_{deep}$ Channel 14 Processed nT/s
612	621	63	Z GEOTEM$_{deep}$ Channel 15 Processed nT/s
622	631	64	Z GEOTEM$_{deep}$ Channel 16 Processed nT/s
632	641	65	Z GEOTEM$_{deep}$ Channel 17 Processed nT/s
642	651	66	Z GEOTEM$_{deep}$ Channel 18 Processed nT/s
652	661	67	Z GEOTEM$_{deep}$ Channel 19 Processed nT/s
662	671	68	Z GEOTEM$_{deep}$ Channel 20 Processed nT/s
672	683	69	X GEOTEM$_{deep}$ Inpulse Channel 1 Processed ppm
684	695	70	X GEOTEM$_{deep}$ Inpulse Channel 2 Processed ppm
696	707	71	X GEOTEM$_{deep}$ Inpulse Channel 3 Processed ppm
708	719	72	X GEOTEM$_{deep}$ Inpulse Channel 4 Processed ppm
720	731	73	X GEOTEM$_{deep}$ Channel 5 Processed ppm
732	743	74	X GEOTEM$_{deep}$ Channel 6 Processed ppm
744	755	75	X GEOTEM$_{deep}$ Channel 7 Processed ppm
756	767	76	X GEOTEM$_{deep}$ Channel 8 Processed ppm
768	779	77	X GEOTEM$_{deep}$ Channel 9 Processed ppm
780	791	78	X GEOTEM$_{deep}$ Channel 10 Processed ppm
792	803	79	X GEOTEM$_{deep}$ Channel 11 Processed ppm
804	815	80	X GEOTEM$_{deep}$ Channel 12 Processed ppm
816	827	81	X GEOTEM$_{deep}$ Channel 13 Processed ppm
828	839	82	X GEOTEM$_{deep}$ Channel 14 Processed ppm
840	851	83	X GEOTEM$_{deep}$ Channel 15 Processed ppm
852	863	84	X GEOTEM$_{deep}$ Channel 16 Processed ppm
864	875	85	X GEOTEM$_{deep}$ Channel 17 Processed ppm
876	887	86	X GEOTEM$_{deep}$ Channel 18 Processed ppm
888	899	87	X GEOTEM$_{deep}$ Channel 19 Processed ppm
900	911	88	X GEOTEM$_{deep}$ Channel 20 Processed ppm
912	923	89	Z GEOTEM$_{deep}$ Inpulse Channel 1 Processed ppm
924	935	90	Z GEOTEM$_{deep}$ Inpulse Channel 2 Processed ppm
936	947	91	Z GEOTEM$_{deep}$ Inpulse Channel 3 Processed ppm
948	959	92	Z GEOTEM$_{deep}$ Inpulse Channel 4 Processed ppm
960	971	93	Z GEOTEM$_{deep}$ Channel 5 Processed ppm
972	983	94	Z GEOTEM$_{deep}$ Channel 6 Processed ppm

984	995	95	Z GEOTEM$_{deep}$ Channel 7 Processed ppm
996	1007	96	Z GEOTEM$_{deep}$ Channel 8 Processed ppm
1008	1019	97	Z GEOTEM$_{deep}$ Channel 9 Processed ppm
1020	1031	98	Z GEOTEM$_{deep}$ Channel 10 Processed ppm
1032	1043	99	Z GEOTEM$_{deep}$ Channel 11 Processed ppm
1044	1055	100	Z GEOTEM$_{deep}$ Channel 12 Processed ppm
1056	1067	101	Z GEOTEM$_{deep}$ Channel 13 Processed ppm
1068	1079	102	Z GEOTEM$_{deep}$ Channel 14 Processed ppm
1080	1091	103	Z GEOTEM$_{deep}$ Channel 15 Processed ppm
1092	1103	104	Z GEOTEM$_{deep}$ Channel 16 Processed ppm
1104	1115	105	Z GEOTEM$_{deep}$ Channel 17 Processed ppm
1116	1127	106	Z GEOTEM$_{deep}$ Channel 18 Processed ppm
1128	1139	107	Z GEOTEM$_{deep}$ Channel 19 Processed ppm
1140	1151	108	Z GEOTEM$_{deep}$ Channel 20 Processed ppm
1152	1161	109	X GEOTEM$_{deep}$ Inpulse Channel 1 Raw nT/s
1162	1171	110	X GEOTEM$_{deep}$ Inpulse Channel 2 Raw nT/s
1172	1181	111	X GEOTEM$_{deep}$ Inpulse Channel 3 Raw nT/s
1182	1191	112	X GEOTEM$_{deep}$ Inpulse Channel 4 Raw nT/s
1192	1201	113	X GEOTEM$_{deep}$ Channel 5 Raw nT/s
1202	1211	114	X GEOTEM$_{deep}$ Channel 6 Raw nT/s
1212	1221	115	X GEOTEM$_{deep}$ Channel 7 Raw nT/s
1222	1231	116	X GEOTEM$_{deep}$ Channel 8 Raw nT/s
1232	1241	117	X GEOTEM$_{deep}$ Channel 9 Raw nT/s
1242	1251	118	X GEOTEM$_{deep}$ Channel 10 Raw nT/s
1252	1261	119	X GEOTEM$_{deep}$ Channel 11 Raw nT/s
1262	1271	120	X GEOTEM$_{deep}$ Channel 12 Raw nT/s
1272	1281	121	X GEOTEM$_{deep}$ Channel 13 Raw nT/s
1282	1291	122	X GEOTEM$_{deep}$ Channel 14 Raw nT/s
1292	1301	123	X GEOTEM$_{deep}$ Channel 15 Raw nT/s
1302	1311	124	X GEOTEM$_{deep}$ Channel 16 Raw nT/s
1312	1321	125	X GEOTEM$_{deep}$ Channel 17 Raw nT/s
1322	1331	126	X GEOTEM$_{deep}$ Channel 18 Raw nT/s
1332	1341	127	X GEOTEM$_{deep}$ Channel 19 Raw nT/s
1342	1351	128	X GEOTEM$_{deep}$ Channel 20 Raw nT/s
1352	1361	129	Y GEOTEM$_{deep}$ Inpulse Channel 1 Raw nT/s
1362	1371	130	Y GEOTEM$_{deep}$ Inpulse Channel 2 Raw nT/s
1372	1381	131	Y GEOTEM$_{deep}$ Inpulse Channel 3 Raw nT/s
1382	1391	132	Y GEOTEM$_{deep}$ Inpulse Channel 4 Raw nT/s
1392	1401	133	Y GEOTEM$_{deep}$ Channel 5 Raw nT/s
1402	1411	134	Y GEOTEM$_{deep}$ Channel 6 Raw nT/s
1412	1421	135	Y GEOTEM$_{deep}$ Channel 7 Raw nT/s
1422	1431	136	Y GEOTEM$_{deep}$ Channel 8 Raw nT/s
1432	1441	137	Y GEOTEM$_{deep}$ Channel 9 Raw nT/s
1442	1451	138	Y GEOTEM$_{deep}$ Channel 10 Raw nT/s
1452	1461	139	Y GEOTEM$_{deep}$ Channel 11 Raw nT/s
1462	1471	140	Y GEOTEM$_{deep}$ Channel 12 Raw nT/s
1472	1481	141	Y GEOTEM$_{deep}$ Channel 13 Raw nT/s
1482	1491	142	Y GEOTEM$_{deep}$ Channel 14 Raw nT/s
1492	1501	143	Y GEOTEM$_{deep}$ Channel 15 Raw nT/s

1502	1511	144	Y GEOTEM$_{deep}$ Channel 16 Raw nT/s
1512	1521	145	Y GEOTEM$_{deep}$ Channel 17 Raw nT/s
1522	1531	146	Y GEOTEM$_{deep}$ Channel 18 Raw nT/s
1532	1541	147	Y GEOTEM$_{deep}$ Channel 19 Raw nT/s
1542	1551	148	Y GEOTEM$_{deep}$ Channel 20 Raw nT/s
1552	1561	149	Z GEOTEM$_{deep}$ Inpulse Channel 1 Raw nT/s
1562	1571	150	Z GEOTEM$_{deep}$ Inpulse Channel 2 Raw nT/s
1572	1581	151	Z GEOTEM$_{deep}$ Inpulse Channel 3 Raw nT/s
1582	1591	152	Z GEOTEM$_{deep}$ Inpulse Channel 4 Raw nT/s
1592	1601	153	Z GEOTEM$_{deep}$ Channel 5 Raw nT/s
1602	1611	154	Z GEOTEM$_{deep}$ Channel 6 Raw nT/s
1612	1621	155	Z GEOTEM$_{deep}$ Channel 7 Raw nT/s
1622	1631	156	Z GEOTEM$_{deep}$ Channel 8 Raw nT/s
1632	1641	157	Z GEOTEM$_{deep}$ Channel 9 Raw nT/s
1642	1651	158	Z GEOTEM$_{deep}$ Channel 10 Raw nT/s
1652	1661	159	Z GEOTEM$_{deep}$ Channel 11 Raw nT/s
1662	1671	160	Z GEOTEM$_{deep}$ Channel 12 Raw nT/s
1672	1681	161	Z GEOTEM$_{deep}$ Channel 13 Raw nT/s
1682	1691	162	Z GEOTEM$_{deep}$ Channel 14 Raw nT/s
1692	1701	163	Z GEOTEM$_{deep}$ Channel 15 Raw nT/s
1702	1711	164	Z GEOTEM$_{deep}$ Channel 16 Raw nT/s
1712	1721	165	Z GEOTEM$_{deep}$ Channel 17 Raw nT/s
1722	1731	166	Z GEOTEM$_{deep}$ Channel 18 Raw nT/s
1732	1741	167	Z GEOTEM$_{deep}$ Channel 19 Raw nT/s
1742	1751	168	Z GEOTEM$_{deep}$ Channel 20 Raw nT/s
1752	1761	169	X GEOTEM$_{deep}$ Channel 5 Processed Alt corrected nT/s
1762	1771	170	X GEOTEM$_{deep}$ Channel 6 Processed Alt corrected nT/s
1772	1781	171	X GEOTEM$_{deep}$ Channel 7 Processed Alt corrected nT/s
1782	1791	172	X GEOTEM$_{deep}$ Channel 8 Processed Alt corrected nT/s
1792	1801	173	X GEOTEM$_{deep}$ Channel 9 Processed Alt corrected nT/s
1802	1811	174	X GEOTEM$_{deep}$ Channel 10 Processed Alt corrected nT/s
1812	1821	175	X GEOTEM$_{deep}$ Channel 11 Processed Alt corrected nT/s
1822	1831	176	X GEOTEM$_{deep}$ Channel 12 Processed Alt corrected nT/s
1832	1841	177	X GEOTEM$_{deep}$ Channel 13 Processed Alt corrected nT/s
1842	1851	178	X GEOTEM$_{deep}$ Channel 14 Processed Alt corrected nT/s
1852	1861	179	X GEOTEM$_{deep}$ Channel 15 Processed Alt corrected nT/s
1862	1871	180	X GEOTEM$_{deep}$ Channel 16 Processed Alt corrected nT/s
1872	1881	181	X GEOTEM$_{deep}$ Channel 17 Processed Alt corrected nT/s
1882	1891	182	X GEOTEM$_{deep}$ Channel 18 Processed Alt corrected nT/s
1892	1901	183	X GEOTEM$_{deep}$ Channel 19 Processed Alt corrected nT/s
1902	1911	184	X GEOTEM$_{deep}$ Channel 20 Processed Alt corrected nT/s
1912	1921	185	Z GEOTEM$_{deep}$ Channel 5 Processed Alt corrected nT/s
1922	1931	186	Z GEOTEM$_{deep}$ Channel 6 Processed Alt corrected nT/s
1932	1941	187	Z GEOTEM$_{deep}$ Channel 7 Processed Alt corrected nT/s
1942	1951	188	Z GEOTEM$_{deep}$ Channel 8 Processed Alt corrected nT/s
1952	1961	189	Z GEOTEM$_{deep}$ Channel 9 Processed Alt corrected nT/s
1962	1971	190	Z GEOTEM$_{deep}$ Channel 10 Processed Alt corrected nT/s
1972	1981	191	Z GEOTEM$_{deep}$ Channel 11 Processed Alt corrected nT/s
1982	1991	192	Z GEOTEM$_{deep}$ Channel 12 Processed Alt corrected nT/s

1992	2001	193	Z GEOTEM$_{deep}$ Channel 13 Processed Alt corrected nT/s
2002	2011	194	Z GEOTEM$_{deep}$ Channel 14 Processed Alt corrected nT/s
2012	2021	195	Z GEOTEM$_{deep}$ Channel 15 Processed Alt corrected nT/s
2022	2031	196	Z GEOTEM$_{deep}$ Channel 16 Processed Alt corrected nT/s
2032	2041	197	Z GEOTEM$_{deep}$ Channel 17 Processed Alt corrected nT/s
2042	2051	198	Z GEOTEM$_{deep}$ Channel 18 Processed Alt corrected nT/s
2052	2061	199	Z GEOTEM$_{deep}$ Channel 19 Processed Alt corrected nT/s
2062	2071	200	Z GEOTEM$_{deep}$ Channel 20 Processed Alt corrected nT/s
2072	2081	201	X B Field GEOTEM$_{deep}$ Inpulse Channel 1 Processed pT
2082	2091	202	X B Field GEOTEM$_{deep}$ Inpulse Channel 2 Processed pT
2092	2101	203	X B Field GEOTEM$_{deep}$ Inpulse Channel 3 Processed pT
2102	2111	204	X B Field GEOTEM$_{deep}$ Inpulse Channel 4 Processed pT
2112	2121	205	X B Field GEOTEM$_{deep}$ Channel 5 Processed pT
2122	2131	206	X B Field GEOTEM$_{deep}$ Channel 6 Processed pT
2132	2141	207	X B Field GEOTEM$_{deep}$ Channel 7 Processed pT
2142	2151	208	X B Field GEOTEM$_{deep}$ Channel 8 Processed pT
2152	2161	209	X B Field GEOTEM$_{deep}$ Channel 9 Processed pT
2162	2171	210	X B Field GEOTEM$_{deep}$ Channel 10 Processed pT
2172	2181	211	X B Field GEOTEM$_{deep}$ Channel 11 Processed pT
2182	2191	212	X B Field GEOTEM$_{deep}$ Channel 12 Processed pT
2192	2201	213	X B Field GEOTEM$_{deep}$ Channel 13 Processed pT
2202	2211	214	X B Field GEOTEM$_{deep}$ Channel 14 Processed pT
2212	2221	215	X B Field GEOTEM$_{deep}$ Channel 15 Processed pT
2222	2231	216	X B Field GEOTEM$_{deep}$ Channel 16 Processed pT
2232	2241	217	X B Field GEOTEM$_{deep}$ Channel 17 Processed pT
2242	2251	218	X B Field GEOTEM$_{deep}$ Channel 18 Processed pT
2252	2261	219	X B Field GEOTEM$_{deep}$ Channel 19 Processed pT
2262	2271	220	X B Field GEOTEM$_{deep}$ Channel 20 Processed pT
2272	2281	221	Y B Field GEOTEM$_{deep}$ Inpulse Channel 1 Processed pT
2282	2291	222	Y B Field GEOTEM$_{deep}$ Inpulse Channel 2 Processed pT
2292	2301	223	Y B Field GEOTEM$_{deep}$ Inpulse Channel 3 Processed pT
2302	2311	224	Y B Field GEOTEM$_{deep}$ Inpulse Channel 4 Processed pT
2312	2321	225	Y B Field GEOTEM$_{deep}$ Channel 5 Processed pT
2322	2331	226	Y B Field GEOTEM$_{deep}$ Channel 6 Processed pT
2332	2341	227	Y B Field GEOTEM$_{deep}$ Channel 7 Processed pT
2342	2351	228	Y B Field GEOTEM$_{deep}$ Channel 8 Processed pT
2352	2361	229	Y B Field GEOTEM$_{deep}$ Channel 9 Processed pT
2362	2371	230	Y B Field GEOTEM$_{deep}$ Channel 10 Processed pT
2372	2381	231	Y B Field GEOTEM$_{deep}$ Channel 11 Processed pT
2382	2391	232	Y B Field GEOTEM$_{deep}$ Channel 12 Processed pT
2392	2401	233	Y B Field GEOTEM$_{deep}$ Channel 13 Processed pT
2402	2411	234	Y B Field GEOTEM$_{deep}$ Channel 14 Processed pT
2412	2421	235	Y B Field GEOTEM$_{deep}$ Channel 15 Processed pT
2422	2431	236	Y B Field GEOTEM$_{deep}$ Channel 16 Processed pT
2432	2441	237	Y B Field GEOTEM$_{deep}$ Channel 17 Processed pT
2442	2451	238	Y B Field GEOTEM$_{deep}$ Channel 18 Processed pT
2452	2461	239	Y B Field GEOTEM$_{deep}$ Channel 19 Processed pT
2462	2471	240	Y B Field GEOTEM$_{deep}$ Channel 20 Processed pT
2472	2481	241	Z B Field GEOTEM$_{deep}$ Inpulse Channel 1 Processed pT

2482	2491	242	Z B Field GEOTEM$_{deep}$ Inpulse Channel 2 Processed pT
2492	2501	243	Z B Field GEOTEM$_{deep}$ Inpulse Channel 3 Processed pT
2502	2511	244	Z B Field GEOTEM$_{deep}$ Inpulse Channel 4 Processed pT
2512	2521	245	Z B Field GEOTEM$_{deep}$ Channel 5 Processed pT
2522	2531	246	Z B Field GEOTEM$_{deep}$ Channel 6 Processed pT
2532	2541	247	Z B Field GEOTEM$_{deep}$ Channel 7 Processed pT
2542	2551	248	Z B Field GEOTEM$_{deep}$ Channel 8 Processed pT
2552	2561	249	Z B Field GEOTEM$_{deep}$ Channel 9 Processed pT
2562	2571	250	Z B Field GEOTEM$_{deep}$ Channel 10 Processed pT
2572	2581	251	Z B Field GEOTEM$_{deep}$ Channel 11 Processed pT
2582	2591	252	Z B Field GEOTEM$_{deep}$ Channel 12 Processed pT
2592	2601	253	Z B Field GEOTEM$_{deep}$ Channel 13 Processed pT
2602	2611	254	Z B Field GEOTEM$_{deep}$ Channel 14 Processed pT
2612	2621	255	Z B Field GEOTEM$_{deep}$ Channel 15 Processed pT
2622	2631	256	Z B Field GEOTEM$_{deep}$ Channel 16 Processed pT
2632	2641	257	Z B Field GEOTEM$_{deep}$ Channel 17 Processed pT
2642	2651	258	Z B Field GEOTEM$_{deep}$ Channel 18 Processed pT
2652	2661	259	Z B Field GEOTEM$_{deep}$ Channel 19 Processed pT
2662	2671	260	Z B Field GEOTEM$_{deep}$ Channel 20 Processed pT
2672	2680	261	RadAlt -m
2681	2689	262	Magnetics nT
2690	2698	263	GPSHeight -m
2699	2707	264	Barometer -m
2708	2716	265	Amplitude Decay Index -X
2717	2725	266	Amplitude Decay Index -Y
2726	2735	267	50 Hz X coil monitor microvolts

5. GEOTEM BACKGROUND INFORMATION

5.1 The GEOTEM$_{DEEP}$® Multi-Coil System

GEOTEM$_{DEEP}$® is a time domain towed bird electromagnetic system incorporating a high speed EM receiver. The primary electromagnetic pulses are created by a series of discontinuous half-sine current pulses fed into a multi turn transmitting loop surrounding the aircraft and fixed to the nose, tail and wing tips. The pulse repetition rate is 25 Hz (40 bipolar pulses per second).

The EM sensor is an orthogonal set of coils mounted in a "bird", towed behind the aircraft on a cable. The cable is demagnetised to reduce noise levels. Three coil orientations are available. The X component has a horizontal axis in the direction of flight, and the Y component with a lateral horizontal component. The Z component has a vertical axis, which is coplanar with the transmitter coil.

Time-domain airborne electromagnetic systems have historically measured the in-line horizontal (X) component using a coaxial receiver coil. New versions of the electromagnetic systems are designed to collect two additional components (the vertical component (Z) and the lateral horizontal component (Y)) to provide greater diagnostic information. The three components, X, Y and Z can be combined to give the "energy envelope" of the response. Due to asymmetry in the transmitter and receiver coil geometry, the shapes of the component profiles depend on flight direction, the most sensitive component being X component.

In areas where lithological strike is near horizontal, the Z component response provides greater signal-to-noise due to greater coupling. In comparison, the X coils couple best with vertical structures striking perpendicular to the flight direction. In a laterally symmetric environments, the symmetry implies that the Y component will be zero; hence a non-zero y-component indicates lateral inhomogeneity.

In the interpretation of discrete conductors, the Z component data may be used to ascertain the dip and depth to the conductor using simple rules of thumb. The response of the Y component can be used to ascertain the strike direction and lateral offset of the target respectively.

Having the Y and Z component data increases the total response when the profile line has not traversed the target. This increases the possibility of detecting a target located between adjacent flight lines or beyond a survey area.

Each primary current pulse may induce eddy currents in subsurface conductors which decay following cessation of each pulse. Any decaying earth currents can induce voltages in the receiver coils which are proportional to the electromagnetic field. These voltages are sampled over 20 time gates. The centres and widths of these gates are variable and may be placed anywhere within or outside the transmitter pulse.

The time varying EM signals received at the sensor pass through anti-aliasing filters and are then digitised with an A/D converter. The digital data stream from the A/D converter passes into an array processor where all the numerically intensive processing tasks are carried out. The array processor is under control of a multi-tasking minicomputer. The on-board processing sequence is as follows:

<u>Transient Analysis</u>: Transient analysis enables the separation of noise from signal in real time.

<u>Digital Stacking</u>: The stacking of transients to produce 1 recorded reading, of which 4 are recorded every second.

<u>Windowing of Data</u>: The transient is initially sampled over 128 time windows which are then binned to form 20 channels.

5.2 System Calibration

All checks and adjustments are performed at high altitude at the start of each flight to allow for automatic compensation and calibration at survey altitude. The calibrations and compensations are as follows:

5.2.1 Compensation

During the flight, the transmitter creates eddy currents within the structure of the aircraft that have measurable effects at the receiver coil. Compensation for this signal is effected numerically within the receiver by a statistical analysis of the signal at the bird in the absence of ground response (by flying at an altitude in excess of 600 m above ground level). The observed signal is used to define a compensation signal that is removed from the observed signal to produce a null and thus effectively buck out any response due to changing geometry between receiver and transmitter (ie between the bird and the aircraft);

5.2.2 Normalisation

All EM response channels are automatically calibrated and reduced to parts per million of the primary field in the receiver.

6. Appendix. RMS Thermal Paper Storage Instruction

Storage:

Ambient Temperature:	Less than 25°C
Relative Humidity:	Less than 65%
Storage Location:	In darkness before and after exposure.

Under these conditions, the paper should retain its characteristics and the printed images will remain legible for at least 5 years, although in the case of blue image paper, there may be some slight fading.

To Eliminate Premature Paper Development:

- Colour development begins at temperatures between 70 to 100°C, and reaches saturation density between 80 and 120°C. Premature development of the paper may occur at lower temperatures, and particularly if the humidity is greater than 65%.
  eg. If the paper is stored for 24 hours at a temperature of 60°C, some development may occur. Or if the paper is stored for 24 hours at a temperature of 45°C when the relative humidity is 90%, development may also occur.

- Avoid use of solvent-type adhesives. Adhesives containing volatile organic solvents such as alcohol, ester, ketone, etc causes colour formation and therefore rubber-type adhesives etc should not be used. Starch, PVA and CMC type adhesives are recommended.

- Frictional heat generated by rubbing a finger nail or sharp object over the surface will cause images to develop.

- Thermal paper will develop colour if brought into contact with freshly processed Diazo copying paper.

To Eliminate Paper Fading:

- Thermal paper will turn yellow, and blue printed images will fade if exposed to direct sunlight or to fluorescent lighting for long periods. File exposed paper in the dark immediately after exposure. Do not store paper near windows.

- Prolonged contact with PVC film containing plasticisers such as ester phthalate will reduce the image forming ability of the paper and cause printed images to fade. We recommend that files made of polyethylene, polypropylene, polyester, etc be used.

- Self-adhesive cellophane tapes containing an alcohol type plasticiser will cause the image to fade. Double-sided adhesive tape is recommended for use instead of paste.

- Handling thermal paper with dirty or sweaty fingers may cause images to fade.

- Do not store developed paper with the sensitised surfaces touching as images might be transferred from one sheet to another.